



Minerva Access is the Institutional Repository of The University of Melbourne

Author/s:

Sabaroedin, K;Razi, A;Chopra, S;Tran, N;Pozaruk, A;Chen, Z;Finlay, A;Nelson, B;Allott, K;Alvarez-Jimenez, M;Graham, J;Yuen, HP;Harrigan, S;Cropley, V;Sharma, S;Saluja, B;Williams, R;Pantelis, C;Wood, SJ;O'Donoghue, B;Francey, S;McGorry, P;Aquino, K;Fornito, A

Title:

Frontostriathalamic effective connectivity and dopaminergic function in the psychosis continuum

Date:

2023-01-01

Citation:

Sabaroedin, K., Razi, A., Chopra, S., Tran, N., Pozaruk, A., Chen, Z., Finlay, A., Nelson, B., Allott, K., Alvarez-Jimenez, M., Graham, J., Yuen, H. P., Harrigan, S., Cropley, V., Sharma, S., Saluja, B., Williams, R., Pantelis, C., Wood, S. J. ,... Fornito, A. (2023). Frontostriathalamic effective connectivity and dopaminergic function in the psychosis continuum. *Brain*, 146 (1), pp.372-386. <https://doi.org/10.1093/brain/awac018>.

Persistent Link:

<https://hdl.handle.net/11343/301592>

License:

[CC BY-NC](#)

1 Frontostriathalamic effective connectivity and dopaminergic 2 function in the psychosis continuum

3 Kristina Sabaroedin,¹ Adeel Razi,^{1,2,3} Sidhant Chopra,¹ Nancy Tran,¹ Andrii Pozaruk,² Zhaolin Chen,² Amy
4 Finlay,¹ Barnaby Nelson,^{4,5} Kelly Allott,^{4,5} Mario Alvarez-Jimenez,^{4,5} Jessica Graham,^{4,5} Hok P. Yuen,^{4,5} Susy
5 Harrigan,^{6,7} Vanessa Cropley,⁸ Sujit Sharma,⁹ Bharat Saluja,⁹ Rob Williams,¹⁰ Christos Pantelis,^{8,11} Stephen
6 J. Wood,^{4,5,12} Brian O'Donoghue,^{4,5} Shona Francey,^{4,5} Patrick McGorry,^{4,5} Kevin Aquino^{1,2} and Alex
7 Fornito^{1,2}

8 1 Turner Institute for Brain and Mental Health, School of Psychological Sciences, Monash University,
9 Clayton, Victoria 3800, Australia

10 2 Monash Biomedical Imaging, Monash University, Clayton, Victoria 3800, Australia

11 3 Wellcome Centre for Human Neuroimaging, University College, London WC1N 3AR, UK

12 4 Orygen, Parkville, Victoria 3052, Australia

13 5 Centre for Youth Mental Health, The University of Melbourne, Parkville, Victoria 3052, Australia

14 6 Department of Social Work, Monash University, Victoria 3800, Australia

15 7 Melbourne School of Population and Global Health, The University of Melbourne, Parkville, Victoria
16 3010, Australia

17 8 Melbourne Neuropsychiatry Centre, Department of Psychiatry, The University of Melbourne &
18 Melbourne Health, Parkville, Victoria 3010, Australia

19 9 Monash Health, Dandenong, Victoria, 3175, Australia

20 10 The University of Melbourne, Parkville, Victoria 3010, Australia

21 11 The Florey Institute for Neuroscience and Mental Health, The University of Melbourne, Parkville,
22 Victoria 3052, Australia

23 12 School of Psychology, University of Birmingham, Edgbaston, Birmingham B15 2TT, UK

24
25 Correspondence to: Kristina Sabaroedin

26 Turner Institute for Brain and Mental Health

27 770 Blackburn Road, Clayton

28 Victoria 3168, Australia

29 E-mail: Kristina.Sabaroedin@monash.edu

30 **Running title:** Frontostriatal connectivity in psychosis

1 Abstract

2 Dysfunction of fronto-striato-thalamic (FST) circuits is thought to contribute to dopaminergic
3 dysfunction and symptom onset in psychosis, but it remains unclear whether this dysfunction is driven
4 by aberrant bottom-up subcortical signaling or impaired top-down cortical regulation.

5 We used spectral dynamic causal modelling of resting-state functional magnetic resonance imaging
6 (fMRI) to characterize the effective connectivity of dorsal and ventral FST circuits in a sample of 46
7 antipsychotic-naïve first-episode psychosis patients and 23 controls and an independent sample of 36
8 patients with established schizophrenia patients and 100 controls. We also investigated the association
9 between FST effective connectivity and striatal [¹⁸F]DOPA uptake in an independent healthy cohort of 33
10 individuals who underwent concurrent fMRI and positron emission tomography.

11 Using a posterior probability threshold of 0.95, we found that midbrain and thalamic connectivity were
12 implicated as dysfunctional across both patient groups. Dysconnectivity in first-episode psychosis
13 patients was mainly restricted to the subcortex, with positive symptom severity being associated with
14 midbrain connectivity. Dysconnectivity between the cortex and subcortical systems was only apparent in
15 established schizophrenia patients. In the healthy [¹⁸F]DOPA cohort, we found that striatal dopamine
16 synthesis capacity was associated with the effective connectivity of nigrostriatal and striatothalamic
17 pathways, implicating similar circuits to those associated with psychotic symptom severity in patients.

18 Overall, our findings indicate that subcortical dysconnectivity is evident in the early stages of psychosis,
19 that cortical dysfunction may emerge later in the illness, and that nigrostriatal and striatothalamic
20 signaling are closely related to striatal dopamine synthesis capacity, which is a robust marker for
21 psychosis.

22 **Keywords:** effective connectivity; dopamine; frontostriatal; psychosis; schizophrenia

23 **Abbreviations:** DCM: dynamic causal model; dlPFC: dorsolateral prefrontal cortex; FEP: first-episode
24 psychosis; FST: fronto-striato-thalamic; PEB: parametric empirical bayes; Pp: posterior probability; SN:
25 substantia nigra; vmPFC: ventromedial prefrontal cortex; VTA: ventral tegmental area

26

27

1 Introduction

2 Dysfunction of fronto-striato-thalamic (FST) circuits linking the caudate and putamen with the
3 prefrontal cortex is thought to be central to the emergence of psychotic symptoms.¹⁻⁶ Two such
4 circuits are particularly relevant: 1) a ventral ‘limbic’ system involved in emotional and reward
5 processing, which connects the orbital and ventromedial prefrontal cortices and subcortical
6 limbic structures (e.g., hippocampus and amygdala) with the nucleus accumbens (NAcc); and 2)
7 a dorsal ‘associative’ system, which links the dorsolateral prefrontal cortex (dlPFC) with the
8 dorsal striatum, and subserves associative learning and executive functions.^{1,7} Feedback loops
9 passing through the pallidum and the thalamus connect both circuits back to the cortex.¹

10 The striatum is a major target for dopamine projections from the ventral tegmental area
11 (VTA) and substantia nigra (SN), with the ventral and the dorsal regions respectively forming
12 part of the mesolimbic and nigrostriatal pathways.⁸ Dysregulated dopamine signaling is proposed
13 to contribute to psychosis onset by influencing the capacity of the striatum to filter and relay
14 information to the thalamus, thus affecting broader FST function.⁹ In-vivo positron emission
15 tomography (PET) has revealed elevated presynaptic dopamine synthesis capacity, measured
16 using 3,4-dihydroxy-6-[¹⁸F]-fluoro-L-phenylalanine ([¹⁸F]DOPA), in the dorsal striatum of at-
17 risk groups, especially in individuals who transition to psychosis.^{10,11} Increased dopamine
18 binding and release in the dorsal striatum have also been shown in psychosis patients and at-risk
19 individuals.^{12,13} Moreover, [¹⁸F]DOPA elevations in the ventral striatum of schizophrenia
20 patients and of at-risk individuals have been reported.^{14,15} In parallel, resting-state functional
21 magnetic resonance imaging (fMRI) studies have identified reduced functional connectivity
22 between the dorsal striatum, thalamus, and dlPFC in first episode psychosis (FEP) patients, their
23 unaffected first-degree relatives, at-risk individuals, chronic unmedicated patients, and healthy

1 people with psychosis-like experiences.^{2-5,16,17} Increased functional connectivity between the
2 ventral striatum, limbic regions, anterior cingulate cortex, ventromedial prefrontal and
3 orbitofrontal cortices has also been found in these groups.^{2,18-20} Correlations between striatal
4 [¹⁸F]DOPA activation of prefrontal and medial temporal areas have been reported in early and
5 chronic stages of psychotic illness.²¹⁻²³

6 Functional connectivity quantifies statistical dependencies between regional activity and does
7 not distinguish causal interactions. It is therefore unclear whether FST dysfunction in psychosis arises
8 from altered bottom-up signaling or disrupted top-down regulation of subcortical systems. Evidence for
9 a primary bottom-up pathology comes from reports of aberrant molecular function, activity, and
10 functional connectivity of the midbrain across at-risk and schizophrenia groups.²⁴⁻²⁶ Others have
11 proposed, largely based on ex-vivo and preclinical findings, that subcortical changes are secondary to
12 deficient top-down control of midbrain neurons, which is caused by GABA/glutamate imbalance in the
13 cortex or hippocampus.^{9,27,28} However, in-vivo imaging findings have been mixed, with reports of
14 increased, decreased, or no changes in prefrontal excitatory or inhibitory metabolites in FEP²⁹⁻³³ and
15 people with established schizophrenia.^{30,31,34,35}

16 Top-down and bottom-up interactions between distinct elements of FST systems can be
17 disentangled through models of effective connectivity. Effective connectivity refers to the causal
18 influence that one neural system exerts over another³⁶ which can be estimated from fMRI data using
19 dynamic causal modelling (DCM). DCM uses a Bayesian framework for optimizing a generative model of
20 directed, or causal, influences between regions comprising a distributed neural system.³⁶ In DCM, inter-
21 regional connections are referred to as extrinsic connections³⁷ and they can be used to infer top-down
22 influences from cortical to subcortical areas or bottom-up subcortical-to-cortical interactions. Another
23 important feature of DCM is that it allows the investigation of the intrinsic functioning of a brain region
24 through the estimation of recurrent inhibition, modelled as a self-connection, which can uncover intra-
25 regional pathology.³⁷ Here, we used spectral DCM DCM³⁸ of resting-state fMRI data to characterize
26 disruptions of extrinsic and recurrent intrinsic effective connectivity within dorsal and ventral FST
27 systems in antipsychotic-naïve FEP patients and people with established schizophrenia (SCZ), as well as
28 associations with psychotic symptoms, which have historically been linked to FST dysfunction.³⁹ In an
29 independent healthy cohort who underwent concurrent fMRI and [¹⁸F]DOPA PET we then identified the
30 specific FST connections that are associated with dorsal and ventral striatal [¹⁸F]DOPA levels. This
31 approach allowed us to cross-sectionally map effective dysconnectivity of FST circuits across different
32 illness stages and to identify putative directed influences associated with striatal dopamine synthesis
33 capacity, a robust marker of illness risk.^{10,40,41}

1 **Materials and methods**

2 **Participants**

3 We examined three independent cohorts: (1) a FEP cohort comprising antipsychotic-naïve patients
4 within six months of psychosis onset and healthy controls;⁴² (2) a SCZ cohort comprising schizophrenia
5 patients and healthy controls obtained through the UCLA Consortium for Neuropsychiatric Phenomics
6 open dataset;⁴³ and (3) an [¹⁸F]DOPA cohort comprising healthy participants recruited from the
7 community who underwent concurrent PET/fMRI scans. The FEP and SCZ cohorts allowed us to examine
8 FST effective connectivity at distinct illness stages, while the [¹⁸F]DOPA cohort allowed us to identify
9 specific connections associated with striatal dopamine synthesis capacity. Separate analyses were also
10 performed for a subgroup of the FEP cohort with a schizophrenia diagnosis (FEP-SCZ) to examine
11 whether there were diagnosis-specific effects within the FEP group. Group numbers and demographic
12 details are provided in Table 1. The recruitment of our FEP cohort and controls, and the [¹⁸F]DOPA
13 cohort was in accordance with the Melbourne Health Human Research Ethics Committee (reference
14 numbers 2007.616 and 1443066.1). Below are the recruitment details for each of our cohort. Detailed
15 description of the number of recruited participants excluded from our analyses are outlined in
16 Supplementary Material.

17 **First-episode psychosis (FEP)**

18 Participants were aged 15–25 years, presenting with FEP to an early psychosis intervention centre at
19 Orygen Youth Health, Melbourne, Australia.⁴² FEP was defined as fulfilling Structured Clinical Interview
20 for DSM-5 (SCID-5) criteria for a psychotic disorder. Patients with substance-induced psychosis were
21 excluded in the present study. Healthy controls had no history of psychiatric or neurological illness, as
22 determined by self-reports, SCID, and the Comprehensive Assessment of At-Risk Mental States.
23 Recruitment period occurred from April 2008 until December 2016. All participants provided informed
24 consent. For FEP patients, additional strict inclusion criteria include comprehension of English language,
25 no contraindication to MRI scanning, less than six months of duration of untreated psychosis, living in
26 stable accommodation, low risk to self or others (score of < 5 on the Brief Psychiatric Rating Scale
27 version 4 (BPRS-4) Suicidality and Hostility subscales), and minimal previous exposure to antipsychotic
28 medication (less than 7 days of use or lifetime 1750mg chlorpromazine equivalent exposure). Healthy
29 controls were age matched to patients. Additional exclusion criteria for controls included history of
30 psychiatric or neurological illness in first-degree relatives and current use of psychotropic medications. A
31 total of 46 patients and 23 controls were included in our final analyses. We also analyzed a subsample of
32 FEP patients with schizophrenia diagnoses (FEP-SCZ; $n = 17$) to identify the differences in connectivity
33 based on differential diagnoses.

34 **Established schizophrenia (SCZ)**

35 Data were obtained through the UCLA Consortium for Neuropsychiatric Phenomics (CNP) open
36 dataset.⁴³ The initial sample consisted of 121 right-handed healthy controls and 51 schizophrenia

1 patients aged between 21–50 years old. Healthy controls were excluded if they had a lifetime history of
2 mental illness, including schizophrenia or other psychotic disorders, and bipolar disorders. Healthy
3 controls were also excluded on current diagnosis of major depressive disorder, suicidality, anxiety
4 disorder or attention deficit hyperactivity disorder (ADHD). Additional exclusion criteria for all
5 participants included left-handedness, pregnancy, neurological disease, history of head injury with loss
6 of consciousness or cognitive sequelae, use of psychoactive medications, substance abuse or
7 dependence, and other MRI contraindications (e.g., claustrophobia). SCZ patients were also excluded if
8 they had comorbidity with either bipolar disorder or ADHD. Diagnoses were based on the DSM-IV and
9 SCID-1. All SCZ patients were on stable medication. Mean lifetime chlorpromazine-equivalent dose⁴⁴ for
10 patients with available medication information is 662.51mg (SD = 764.91mg; $n = 28$). No significant
11 correlations between antipsychotic exposure and effective connectivity were identified (i.e., all $p > .05$,
12 corrected). A total of 36 patients and 100 controls were included in our analyses after quality checking.

13 **Healthy [¹⁸F]DOPA cohort**

14 A total of 52 healthy participants aged 18–28 years old were recruited from the community through
15 online advertisements. Recruitment period was between May 2016 until May 2019. Each participant
16 provided informed consent. Exclusion criteria included current or history of psychiatric or neurological
17 illnesses, significant medical history, intellectual disability, and first-degree relative with a mental illness.
18 Participants underwent simultaneous resting-state fMRI and PET imaging with [¹⁸F]DOPA tracer. A total
19 of 33 participants were included in our final analyses.

20 **Symptom measures**

21 Positive symptoms were assessed in patients using the positive subscale of Brief Psychiatric Rating Scale
22 (BPRS) version 4.⁴⁵ The subscales were derived from a five factor solution outlined in Dazzi et al.⁴⁵
23 Psychotic symptom scores were derived from the positive symptom subscale which consists of five
24 items: unusual thought content, suspiciousness, hallucinations, grandiosity, and bizarre behavior.
25 Secondary analyses also considered negative symptoms assessed with the same instrument. The
26 negative symptom subscale consists of three items: blunted affect, emotional withdrawal, and motor
27 retardation. Each item is ranked on a Likert-like scale between 1 to 7, with a score of 1 denoting the
28 absence of a measured symptom.

29 **fMRI acquisition**

30 The scanning acquisition protocol for each participant group is described in the following.

31 **FEP**

32 Whole-brain T2*-weighted echo-planar images (EPIs) and anatomical T1-weighted (T1w) scans were
33 acquired for each participant using a 3T Siemens Trio Tim scanner, equipped with a 32-channel head
34 coil, located at the Royal Children's Hospital in Melbourne, Australia. Participants were instructed to lie
35 still in the scanner while maintaining wakefulness with eyes closed. A total of 234 functional volumes

1 with 37 slices each were acquired using the following parameters: repetition time = 2000ms; echo time
2 = 32ms; flip angle = 90°; field of view = 210mm; slice thickness of 3.5 mm, and 3.3 x 3.3 x 3.55 mm
3 voxels. A total of 176 slices were acquired for each participant's T1-weighted image using an interleaved
4 acquisition using the following parameters: TR = 2.3s; TE = 2.98ms; flip angle of 9°; FOV of 256mm; voxel
5 size of 1.1 x 1.1. x 1.2 mm.

6 **SCZ**

7 The UCLA CNP dataset⁴³ was acquired on one of two Siemens Trio 3T scanners located at the Ahmanson-
8 Lovelace Brain Mapping Center and the Staglin Center for Cognitive Neuroscience at UCLA. Details of the
9 resting-state EPI scan are TR = 2s, TE = 30ms, flip angle = 90°, 4mm slice thickness, 152 volumes with 34
10 slices each. Participants were instructed to keep their eyes open. Details of the T1 scan are TR = 1.9s, TE
11 = 2.26ms, flip angle of 90°, 176 slices with 1mm³ voxels.

12 **[¹⁸F]DOPA**

13 Data were acquired using a 3T Siemens Magnetom Biograph simultaneous MR-PET scanner equipped
14 with a 20-channel head and neck coil at Monash Biomedical Imaging, Melbourne, Australia. Resting-
15 state whole-brain T2*-weighed echo-planar image (EPIs) was also acquired for each subject using an
16 interleaved acquisition with the following parameters: TR = 2.89s; TE = 30ms; 152 volumes with 44 slices
17 per volume; flip angle = 90°; FOV = 190mm; slice thickness = 3mm; voxel size of 3mm³. A high resolution
18 T1-weighted anatomical image was acquired for each subject using an ascending acquisition (176 slices;
19 TR = 1640ms; TE = 2.34ms; flip angle = 8°; field of view (FOV) = 256mm; slice thickness = 1mm; voxel size
20 = 1mm³).

21 **MRI processing**

22 fMRI and T1-weighted data were processed in the same way across all three cohorts using FMRIPREP
23 software version 1.1.1.⁴⁶ Each T1w scan was corrected for non-uniformity in intensity and subsequently
24 skull stripped. Brain surfaces were reconstructed using FreeSurfer version 6.0.1. Tissue masks were
25 generated using FreeSurfer. Spatial normalization of the skull stripped T1w images to the ICBM 152
26 Nonlinear Asymmetrical template version 2009c was performed using a nonlinear registration in ANTs
27 version 2.1.0. Similarly, for each participant, tissue masks were registered from the surface space to the
28 MNI template.

29 EPIs were slice-timed corrected using AFNI version 16.2.07 and realigned to a mean reference
30 image using FSL. EPIs were distortion corrected using fieldmaps (phasediff-based workflow;
31 <https://fmriprep.readthedocs.io/en/stable/api/index.html#sdc-phasediff>). For participants with missing
32 fieldmaps, a "fieldmap-less" distortion correction was performed by co-registering the functional image
33 to the intensity-inverted T1w image constrained with an EPI distortion atlas.⁴⁷ Following distortion
34 correction, EPIs were co-registered with their corresponding T1w using boundary-based registration
35 with nine degrees of freedom using the bregister routine in FreeSurfer. The motion-correcting
36 transformations, field-distortion-correcting warp, EPI-to-T1w transformation, and T1w-to-MNI template

1 warp were concatenated and applied in a single step using ANTs version 2.1.0. In-scanner head motion
2 was defined as excessive according to previously-defined stringent exclusion criteria;⁴⁸ namely, if any of
3 the following were met: 1) mean framewise displacement (FD) > 0.20mm; (2) sum of suprathreshold FD
4 spikes > 20%; and (3) any FD > 5mm. FD was calculated using the root mean squared volume-to-volume
5 displacement of all voxels, derived from the six head motion parameter (3 translations, 3 rotations).⁴⁸
6 ICA-based Automatic Removal of Motion Artifacts (AROMA) was used to generate noise regressors.⁴⁹
7 ICA-AROMA noise components were non-aggressively regressed out from the EPI data. Next, white
8 matter and cerebrospinal fluid signals were estimated from each subject using restricted tissue masks
9 and were removed out from the data via linear regression. A high-pass filter of 200 seconds was the
10 applied to each EPI image prior to spatial smoothing using a Gaussian kernel of 4mm full-width half-
11 maximum implemented using the 3dBlurToFWHM function in AFNI (version 16.2.16). We did not
12 perform global signal regression as DCM incorporates noise parameter estimates that capture
13 observation noise due to scanner and physiological noise^{38,50} and also because it may remove real
14 neuromodulatory fluctuations in neuronal activity, which are of key interest in the present study (for a
15 discussion, see Aquino et al.⁵¹ and Glasser et al.⁵²).

16 **PET acquisition, processing, and analysis**

17 PET data in the [¹⁸F]DOPA group were acquired on a MR-PET Siemens Biograph scanner. All participants
18 received carbidopa (150 mg) and entacapone (400 mg) orally 60 minutes before imaging to reduce the
19 formation of radiolabeled metabolites that can cross the blood-brain barrier and thus confound tracer
20 availability in the striatum.^{53,54} All subjects were administered approximately 150Mbq of [¹⁸F]DOPA via
21 interbolus injection at the start of the PET imaging. Participants were instructed to lie still in the scanner
22 with eyes closed. Participants were instructed to lie still in the scanner with eyes closed.

23 The pseudo-CT attenuation correction method^{55,56} was used to correct PET images during image
24 reconstruction. Dynamic PET images were reconstructed using the Siemens e7tools software with image
25 volume size 344×344×127(2.09×2.09×2.03mm³). The Ordinary Poisson-Ordered Subset Expectation
26 Maximization (OP-OSEM) algorithm (3 iterations, 21 subsets) was used with the point spread function
27 (PSF) for partial volume correction. A 5-mm FWHM Gaussian filter was applied to each 3D image
28 volume. For correction of subject motion, the list mode dataset was first binned into 95 frames
29 consisting of one 30-second background frame and ninety-four 60-second frames. Dynamic motion was
30 corrected based on an image registration approach,⁵⁷ where each frame was registered to the last frame
31 using rigid-body transformation implemented in the FSL toolbox.⁵⁸ The final reconstructed dynamic PET
32 images were registered to the corresponding T1 MPRAGE MRI image. Patlak graphical analysis⁵⁹ was
33 performed using Qmodeling software⁶⁰ to quantify [¹⁸F]DOPA influx rate constants (K_i^{cer} values) for
34 dorsal and ventral striatal regions-of-interest (ROIs)⁶¹ (Supplementary Fig. S1) relative to the
35 cerebellum⁶² in each participant's anatomical space. We only analyzed the left hemisphere consistent
36 with our DCM (see below).

37

1 **Dynamic causal modeling**

2 **Model space selection**

3 Regions of interest (ROIs) spanning the dorsal and ventral FST systems, and the midbrain were selected
4 using stereotactic coordinates of past findings or of peak signals identified using functional connectivity.
5 Effective connectivity explains the change of activity in one region as a function of activity in another
6 region and does not depend on signal correlations between two areas. As such, selecting regions based
7 on functional connectivity peaks does not result in biased ROI selection. We modelled 47 biologically
8 plausible connections, identified through tract tracing or human functional connectivity, between eight
9 ROIs (Fig. 1). The first eigenvariate of time-series of each ROI was extracted and entered into first-level
10 DCM analysis. We focused on the left hemisphere given prior evidence of more consistent functional
11 connectivity effects in left-lateralized FST circuits in patients.^{2,3} Spherical ROIs were created with a radius
12 of 6mm for cortical regions (i.e., dlPFC and vmPFC) and 3.5mm for each subcortical ROI. For vmPFC and
13 thalamus ROIs with centroids that were close to the anatomical or functional boundary of the region, we
14 used an anatomical mask from the FreeSurfer package when extracting the first eigenvariate for the
15 ROIs to exclude signal from neighboring regions. Details of ROI selection for each region are as below.

16 **Nucleus accumbens (NAcc) and dorsal caudate (DC)**

17 For the ventral and dorsal striatum, we seeded the NAcc and DC consistent with our previous works^{2,4,63}
18 using a functional parcellation of the striatum⁶⁴ that was delineated based on a meta-analysis of striatal
19 activation in fMRI and PET studies.⁶⁵ The pallidum, which is the primary output structure of the basal
20 ganglia, was omitted to limit model dimensionality. Its effects will thus be captured through indirect
21 (unmodelled) influences in the DCM.

22 **Dorsolateral prefrontal cortex (dlPFC)**

23 To capture variations associated with risk for psychosis as well as disruptions in clinical groups, the dlPFC
24 ROI was selected based on a peak in which functional connectivity with the DC was reduced in the
25 healthy relatives of FEP patients compared to healthy controls.² This peak overlapped with an area that
26 also showed reduced connectivity in patients.

27 **Ventromedial prefrontal cortex (vmPFC)**

28 To choose a region that was most relevant to the ventral circuit, we chose a peak in the vmPFC that
29 showed strong functional connectivity with the NAcc in an independent cohort of 353 healthy adults.⁴

30 **Thalamus**

31 The thalamus coordinate was selected from a peak in which functional connectivity with the dorsal
32 caudate was reduced in at-risk mental state individuals compared to healthy controls.⁶³

33

1 Hippocampus and amygdala

2 ROIs for these regions were selected using a similar method. Peak coordinates within anatomical masks
 3 for the hippocampus and amygdala were selected in a separate group-level functional connectivity
 4 analysis of each ROIs connectivity with the whole brain in an independent cohort of 353 individuals.⁴ For
 5 the hippocampus, we chose the anterior region, using of a hippocampal mask provided in the FreeSurfer
 6 package.⁶⁶ The anterior hippocampus is a hippocampal region that is most frequently implicated as
 7 dysfunctional in schizophrenia,⁶⁷ and it was defined as the region having the MNI coordinate of less than
 8 $y = -22$.⁶⁸ Similar to the hippocampus, we used an amygdala mask provided in FreeSurfer.

9 Midbrain

10 The midbrain is a challenging area to identify due to the lack of tissue contrast afforded by anatomical
 11 T1 scans. We therefore employed a midbrain mask derived from a comprehensive study of functional
 12 connectivity between the ventral tegmental area (VTA), substantia nigra (SN) and the rest of the brain,
 13 which has been that was validated in two independent datasets.⁶⁹ Due to the coarse resolution of the
 14 functional scans, we combined VTA and SN into one midbrain ROI, which limits our ability to delineate
 15 mesolimbic and nigrostriatal pathways. We selected a functional connectivity signal peak in the same
 16 cohort that was used in the selection of our hippocampal, amygdala, and vmPFC ROIs.

17 Model estimation

18 We modelled effective connectivity in the spectral domain by fitting a complex cross spectral density
 19 using a generative model, parametrized by a power-law model of endogenous fluctuations,
 20 implemented in SPM12 (DCM 12; revision 7487).³⁸ Details are provided in Supplementary Methods.
 21 Briefly, subject-specific first-level analyses were used to estimate directed (causal) influences between
 22 regions (in Hz), and the (inhibitory) recurrent or self-connectivity (i.e., self-inhibition) within each region.

23 Subject-specific connectivity parameters were then passed to a group-level general linear model
 24 (GLM) implemented in the parametric empirical Bayes (PEB) framework to estimate between-subject
 25 variability.⁷⁰ PEB models were run separately for each cohort. FEP and SCZ patients were compared to
 26 their respective control groups. Symptom associations in patients were modelled separately for each
 27 group for each connection in the model space, with both positive and negative symptoms included as
 28 covariates. Associations with [¹⁸F]DOPA were modelled in healthy individuals only, with dorsal and
 29 ventral striatal K_i^{cer} values as covariates. Age, sex, and mean framewise displacement⁷¹ were used as
 30 nuisance covariates for all models to address unequal distributions of sex across groups, as well as age
 31 and head motion as confounding variables. Scanner site was also used as a covariate in the SCZ group.
 32 We only report effects with a posterior probability threshold above 0.95. This threshold is based upon
 33 the differences in model evidence, or marginal likelihood, observed when comparing models with and
 34 without a particular connection. Critically, PEB is a multivariate (Bayesian) GLM in which we fit all model
 35 parameters at once; hence, no correction for multiple comparisons is required. A typical effect size for
 36 effective connectivity between regions is 0.1 Hz.³⁸ Self-connections are inhibitory to reflect activity
 37 decay, with a negative sign indicating reduced self-inhibition (i.e., disinhibition, or slower activity decay)

1 and a positive sign indicating increased self-inhibition (i.e., quicker activity decay). Note that a group
2 difference of 0 Hz in effective connectivity does not imply the absence of that connection in either
3 group, but instead signifies that the groups do not differ in their effective connectivity. A mean
4 connectivity of 0 Hz within a group denotes an absence of effective connectivity, but it does not
5 necessarily imply a lack of anatomical connectivity. Technical details are outlined in Supplementary
6 Methods.

7 **Checks on variance explained**

8 Connectivity methods based on correlations such as functional connectivity depend on covariances
9 between brain regions, which are influenced by observation noise and changes in signal-to-noise ratio.³⁷
10 In contrast to descriptive correlational methods, DCM accounts for noise by modelling observation noise
11 in the data, which includes thermal and physiological noise⁵⁰ (see equations S2 and S3 in Supplementary
12 Methods). The DCM routine also incorporates a diagnostic check to determine the accuracy of model
13 inversion by calculating the percentage of variance explained by the model based on the predicted BOLD
14 signal.⁷² Based on this diagnostic check, we excluded subjects with <75% variance explained by DCM for
15 subsequent analyses following first-level model inversion (details in Supplementary Methods).

16 **Data availability**

17 Data from the UCLA Consortium for Neuropsychiatric Phenomics are available on an open dataset
18 platform on <https://openneuro.org/datasets/ds000030/versions/00016>. Derived data from our FEP and
19 PET cohorts are available from the corresponding author on request.

20 **Results**

21 **Group differences in effective connectivity**

22 **FEP vs. healthy controls**

23 To examine FST disruptions at the earliest signs of illness, before exposure to antipsychotic medication,
24 we first investigated effective connectivity disruptions in antipsychotic-naïve FEP patients relative to
25 healthy controls. Patients showed reduced self-inhibition of VTA/SN, increased self-inhibition of dlPFC,
26 greater inhibitory influence of the thalamus on NAcc, and a greater excitatory influence of the amygdala
27 on NAcc (Fig. 2A; Table 2). The subset of FEP-SCZ patients (Fig. 2B; Table 2) showed similar changes but
28 did not show increased dlPFC self-inhibition. FEP-SCZ patients additionally demonstrated a relative
29 disinhibition of the amygdala, increased excitatory influence of VTA/SN on NAcc, and increased
30 inhibitory influence of VTA/SN and NAcc on hippocampus. Connections between cortical and subcortical
31 ROIs were not implicated as dysfunctional in FEP patients.

32

1 **SCZ vs. healthy controls**

2 We next examined, in an independent sample of patients and controls, whether people with
3 established schizophrenia show similar disruptions of FST effective connectivity to those observed in
4 FEP. As with FEP, we found that SCZ patients showed disinhibition of VTA/SN and a greater inhibitory
5 influence of thalamus on NAcc relative to controls (Fig. 2C; Table 2). SCZ patients also showed increased
6 inhibitory influence of vmPFC on dlPFC, of dlPFC on thalamus, and of thalamus and amygdala on
7 hippocampus. FEP-SCZ patients and SCZ patients both showed altered bottom-up connectivity of the
8 VTA/SN. In FEP-SCZ, these disruptions primarily affected the limbic circuit; in SCZ patients, they affected
9 the dorsal system, with increased inhibitory influence on the dorsal caudate (DC) on VTA/SN and an
10 increased excitatory influence running in the reverse direction, from DC to VTA/SN.

11

12 **Associations with positive symptoms**

13 Having identified both common and distinct disruptions of FST circuitry in FEP and SCZ patients, we next
14 examined the association between specific FST connections (i.e., how much a region influences another)
15 and psychotic symptom severity in both groups.

16 **FEP**

17 Greater positive symptom severity was predominantly associated with subcortical connectivity (Fig. 3A,
18 Table 3). Specifically, more severe symptoms were associated with a relatively stronger influence of
19 VTA/SN on NAcc and amygdala, of NAcc and hippocampus on VTA/SN. More severe symptoms were also
20 associated with a weaker influence of VTA/SN on DC and hippocampus, and with reduced self-inhibition
21 of the amygdala. In cortex, higher positive symptom ratings were associated with weaker influence of
22 dlPFC on vmPFC and weaker self-inhibition of vmPFC.

23 The FEP-SCZ subgroup (Fig. 3B, Table 3) showed similar associations with vmPFC self-inhibition
24 and subcortical connectivity, although associations with hippocampal to VTA/SN connectivity and
25 amygdala self-inhibition were absent. Positive symptom severity was additionally associated with a
26 weaker influence of NAcc on hippocampus, of hippocampus on amygdala, of DC on thalamus, and
27 reduced dlPFC self-inhibition, coupled with a stronger influence of dlPFC on thalamus and stronger
28 thalamic self-inhibition.

29 **SCZ**

30 Both cortical-subcortical and subcortical-cortical influences were associated with positive symptoms in
31 SCZ patients (Fig. 3C, Table 3). Specifically, more severe positive symptoms were associated with a
32 stronger top-down influence of vmPFC on VTA/SN and hippocampus; stronger bottom-up influence of
33 VTA/SN on dlPFC; stronger influence of DC on thalamus and of thalamus on hippocampus; and greater
34 dlPFC self-inhibition. Higher positive symptom ratings were also associated with weaker vmPFC and

1 VTA/SN self-inhibition and a weaker influence of dlPFC on thalamus, thalamus on VTA/SN, VTA/SN on
2 amygdala, hippocampus on vmPFC. Some common connections were implicated in both FEP-SCZ and
3 SCZ patients (i.e., VTA/SN–amygdala, DC–thalamus, dlPFC–thalamus, and dlPFC self-inhibition), albeit
4 with opposing polarity, suggesting that the link between positive symptoms and altered FST effective
5 connectivity varies across illness stages.

6 **Associations with negative symptoms**

7 Associations with negative symptom for FEP, FEP-SCZ, and SCZ patients are presented in Supplementary
8 Fig. S2 and Table S1. Associations between negative symptom severity and amygdala self-inhibition were
9 consistent, albeit with reversed polarity, across the last two groups. Top-down cortical to subcortical
10 connections were associated with negative symptom severity in FEP-SCZ patients, whereas SCZ patients
11 showed associations with bottom-up subcortical to cortical connections. Similar to positive symptoms,
12 negative symptom associations in FEP patients mainly implicated subcortical connections.

13 **Associations with striatal dopamine synthesis capacity**

14 The analysis of clinical patients identified a prominent role for subcortical dysconnectivity in both FEP
15 and SCZ groups. Dopamine dysregulation plays a central role in the genesis of psychotic symptoms^{73–75}
16 and there is robust evidence for elevated pre-synaptic dopamine synthesis capacity, as measured with
17 [¹⁸F]DOPA, in the dorsal striatum of patients and at-risk individuals,^{10,40,41}. Dopaminergic transmission is
18 influenced by, and influences, FST function.^{8,9,76,77} We therefore set out to identify FST circuit elements
19 that are associated with striatal [¹⁸F]DOPA in an independent sample of healthy individuals who
20 underwent concurrent PET-fMRI.

21 **Dorsal striatum**

22 Significant associations with dorsal striatal [¹⁸F]DOPA in healthy individuals largely implicated the
23 thalamus (Fig. 4; Table 4). Specifically, higher [¹⁸F]DOPA was associated with stronger thalamic self-
24 inhibition; stronger thalamic influence over the VTA/SN and DC; stronger amygdala influence over
25 thalamus; and a weaker influence of DC on thalamus. Stronger bottom-up influence of the amygdala on
26 vmPFC was also associated with higher dorsal striatal [¹⁸F]DOPA.

27 **Ventral striatum**

28 Ventral striatal [¹⁸F]DOPA was associated with a distributed set of extrinsic effective connections
29 centered on midbrain and thalamus (Fig. 4; Table 4). Specifically, higher [¹⁸F]DOPA was associated with
30 weaker self-inhibition of NAcc and amygdala, a weaker influence of these two regions on the thalamus,
31 and a stronger influence of hippocampus on thalamus. Ventral striatal [¹⁸F]DOPA was also associated
32 with greater self-inhibition of the VTA/SN; weaker bottom-up influences of VTA/SN on the vmPFC and
33 DC; weaker and stronger top-down influences of DC and hippocampus on VTA/SN, respectively; and
34 greater DC self-inhibition.

1 Discussion

2 FST dysfunction has been identified in psychotic illnesses,^{2-5,16,18-20} but a characterization of how causal
3 influences within these circuits are altered at distinct illness stages has been lacking. Using spectral
4 DCM, we mapped the effective connectivity of dorsal and ventral FST circuits in FEP and established SCZ.
5 Both clinical groups showed consistent disinhibition of VTA/SN and a stronger top-down inhibitory
6 influence of the thalamus on NAcc. Altered top-down connectivity from the cortex to subcortex was only
7 identified in established illness. Positive symptom severity was associated with a relative disinhibition of
8 the VTA/SN in both illness stages. Additional associations were otherwise largely confined to subcortical
9 connectivity in FEP and a distributed set of cortical and subcortical connections in SCZ patients.
10 Concurrent PET-MRI in healthy individuals revealed distinct sets of FST connections associated with
11 dorsal and ventral dopamine synthesis capacity, with DC and striathalamic connectivity associated
12 with both striatal dopamine synthesis and positive symptom severity. Our findings indicate that
13 midbrain dysfunction and subcortical dysconnectivity is prominent in early illness stages, that cortical
14 dysfunction becomes more salient in established illness, and that striathalamic and nigrostriatal
15 connectivity are related to both striatal dopamine synthesis capacity and positive symptom severity in
16 patients.

17 **Effective dysconnectivity of fronto-striato-thalamic circuitry**

18 We observed VTA/SN disinhibition across both illness stages, suggesting that it represents a core feature
19 of FST pathology in psychosis. Midbrain disinhibition is consistent with elevated striatal dopamine
20 synthesis.¹⁰ Given that we found no evidence of disrupted top-down influences on VTA/SN in FEP in our
21 modelled regions, our findings thus suggest that prior reports of elevated striatal dopamine in [¹⁸F]DOPA
22 and other PET studies across different stages of psychosis may be linked to intrinsic dysregulation of the
23 midbrain.^{28,78}

24 Both FEP and SCZ groups also showed increased inhibitory influence of thalamus over NAcc.
25 Excitatory thalamostriatal projections provide feedback for the striatum to maintain bottom-up signaling
26 to thalamus and cortex in support of specific actions or behaviors.⁷⁹ A greater inhibitory influence of
27 thalamus on NAcc in both FEP and SCZ thus implies a dysregulation of the thalamostriatal feedback
28 pathway. Although this dysregulation was not directly tied to VTA/SN function in our findings, animal
29 models suggest that NAcc dysregulation can disinhibit the midbrain in young adult rats.^{28,80} Notably, we
30 have recently found that antipsychotics rapidly and preferentially impact thalamo-striatal and thalamo-
31 cortical functional connectivity in FEP patients,⁸¹ suggesting that a remediation of thalamic interactions
32 with the rest of the brain may be a key therapeutic mechanism.

33 SCZ patients showed increased inhibitory influence of VTA/SN over DC, which may disrupt the
34 capacity of this area to filter information through the FST circuits.^{9,82} SCZ patients also showed increased
35 top-down excitatory influence of DC over VTA/SN, which may reflect a compensatory response to
36 regulate disinhibited signaling from the midbrain. Given that VTA/SN disinhibition was also observed in
37 FEP, our findings suggest that an early bottom-up pathology of the midbrain may evolve to affect striatal

1 function and potentially dysregulate feedback loops within the dorsal FST with illness progression.
2 However, we cannot rule out an effect of medication in the SCZ group and longitudinal data are required
3 to test this hypothesis.

4 In FEP, cortical dysfunction was limited to increased dlPFC self-inhibition. Post-mortem work has
5 identified robust changes in GABAergic neuron function in patients with established schizophrenia,⁸³ but
6 in vivo studies of FEP patients have been inconsistent, with reports of lower, higher, or no differences in
7 prefrontal GABA levels.^{32,33,84,85} Our findings thus suggest that while DLPFC dysfunction is evident early in
8 psychosis, it does not to play a prominent role in broader FST dysfunction.

9 Taken together, our DCM analysis indicates that the early phase of psychosis is associated with
10 prominent dysfunction of subcortical systems, with alterations in cortico-subcortical connectivity
11 emerging in later illness stages. Intrinsic dysfunction of the VTA/SN and dlPFC, and altered thalamic
12 regulation over the NAcc, appear to be stable features of the illness.

13 **Fronto-striato-thalamic connectivity and symptom severity**

14 A primary role for VTA/SN dysregulation in psychosis is supported by our observations of consistent
15 correlations between the connectivity of this region and positive symptom severity across illness
16 stages.^{26,86–88} However, the specific connections implicated varied across the patient groups. In the full
17 FEP cohort, greater positive symptom severity was associated with connectivity between VTA/SN and
18 limbic subcortical regions, which accords with a role for hippocampal–midbrain dysregulation identified
19 in rodent models of psychosis.²⁸ Disinhibition of the vmPFC, another component of the limbic FST
20 system, was negatively associated with positive symptom severity across the FEP, FEP-SCZ, and SCZ
21 patients.^{89,90}

22 Reduced influence of VTA/SN on DC was also associated with greater positive symptom severity
23 in both FEP-SCZ and SCZ patients. When taken with evidence of robust [¹⁸F]DOPA elevations in the DC in
24 early psychosis,^{10,11,41} our findings of intrinsic dysfunction of the midbrain across illness stages (see also
25 references 23–25), and anatomical studies indicating that midbrain afferents to the dorsal striatum
26 primarily originate in the SN,⁸ our results identify a close link between nigrostriatal signaling and the
27 expression of psychotic symptoms.

28 Several additional FST elements were consistently associated with positive symptom severity in
29 both SCZ and FEP-SCZ patients, although the polarity of associations was often reversed between FEP
30 and SCZ groups. This reversal may be due to several factors, including differences in the neural
31 correlates of psychotic symptoms at different illness stages, an effect of medication in the SCZ group, or
32 a combination of both. Dopamine is proposed to regulate neuronal signalling in complex ways, and it is
33 as yet unclear how dopamine levels at different illness stages relate to measures of functional or
34 effective connectivity.^{91,92} Precisely understanding these effects, and the impact of antipsychotic
35 medication, is an important topic for further investigation.

36 There was less consistency across the cohorts with respect to negative symptom associations,
37 with different sets of connections being associated with symptom severity in the FEP and SCZ groups. In

1 general, the SCZ cohort demonstrated associations that were more widespread across the cortical and
2 subcortical regions compared to the FEP and FEP-SCZ groups. Across both FEP and SCZ cohorts, the
3 dlPFC and subcortical limbic regions, including the amygdala and the hippocampus, were generally
4 implicated, consistent with evidence of prefrontal and limbic involvement in this symptom dimension.⁹³⁻
5⁹⁵

6 **Fronto-striato-thalamic connectivity and striatal dopamine synthesis** 7 **capacity**

8 Dorsal and ventral striatal [¹⁸F]DOPA levels were associated with effective connectivity of distinct FST
9 circuit elements. Most associations with dorsal striatum [¹⁸F]DOPA were limited to the dorsal FST circuit
10 and involved the thalamus. Two thalamic connections—an afferent input from DC and the thalamic self-
11 connection—were also associated with positive symptom severity in FEP-SCZ patients. The modulation
12 of cortical and thalamic glutamatergic signals by striatal dopamine controls striatothalamic filtering and
13 information flow to the cortex, which is thought to play a central role in the pathogenesis of psychosis.⁹
14 The close link between striatal [¹⁸F]DOPA and thalamic connectivity that we identify here may be related
15 to evidence that antipsychotics preferentially impact thalamo-striatal and thalamo-cortical functional
16 connectivity in FEP, and can recover FST connectivity following treatment.^{81,96}

17 Bidirectional connectivity between the VTA/SN and DC was associated with dorsal striatal
18 [¹⁸F]DOPA. This connection was identified as dysfunctional in SCZ patients and was correlated with
19 positive symptom severity in both SCZ and FEP-SCZ. This consistency of findings suggests a close link
20 between nigrostriatal signaling, striatal dopamine synthesis capacity, and positive symptom severity in
21 patients. Notably, positive symptom severity in FEP was associated with a reduced influence of VTA/SN
22 on DC, whereas higher dorsal striatal [¹⁸F]DOPA was associated with an increased afferent influence of
23 VTA/SN. Since patients are known to show elevated [¹⁸F]DOPA in the dorsal striatum,^{10,11} one might
24 expect a negative association between striatal [¹⁸F]DOPA and VTA/SN-DC connectivity. One potential
25 explanation is that elevated dopamine levels lead to compensatory changes in circuit function that
26 affect the optimal balance of signaling between different regions, thus resulting in different circuit
27 mechanisms that regulate dopamine levels in the brains of psychotic and non-psychotic individuals.
28 Concurrent PET-fMRI in both patients and controls would help to test this possibility.

29 Connections associated with ventral striatal [¹⁸F]DOPA were distributed across the ventral and
30 dorsal systems. NAcc projections are widely distributed in the midbrain and drive dorsal striatal
31 dopamine levels.⁸ Accordingly, we found that ventral striatal [¹⁸F]DOPA was associated with VTA/SN-DC
32 connectivity and inhibition within both regions. VTA/SN-DC connectivity was also disrupted in SCZ
33 patients and associated with positive symptoms in FEP, suggesting a link between the NAcc's regulation
34 of midbrain activity and dorsal circuit dysfunction in patients.⁹⁷

35

1 **Limitations and future directions**

2 We used independent samples to cross-sectionally characterize effective dysconnectivity across distinct
3 illness stages. This approach offers a test of consistency across cohorts, but inferences about the
4 progression of circuit dysfunction must be confirmed longitudinally, especially given the differences in
5 sample size and symptom severity across the three cohorts.

6 Psychosis is a highly heterogenous syndrome and diagnostic differences in our cohort may
7 potentially complicate interpretation of our results. FST and dopamine dysfunction have been
8 implicated in the onset of psychotic symptoms, regardless of the underlying diagnosis. In our past work,
9 we have identified common disruptions of FST functional connectivity across people with FEP,² first
10 episode mania with psychosis,⁹⁸ at-risk mental state with psychosis,³ and in association with high levels
11 of subclinical schizotypy.^{4,99} Given this evidence for transdiagnostic effects, and that first-episode
12 diagnoses can sometimes be unstable,^{100,101} it is critical to examine the FEP cohort as a group. The
13 similarity in findings obtained with the full FEP and FEP-SCZ sub-groups with respect to subcortical and
14 midbrain dysconnectivity and symptom associations indicate that diagnostic heterogeneity does not
15 make a major contribution to our findings.

16 As the SCZ patients were medicated, the effects of antipsychotics on the brain should also be
17 considered when interpreting the findings.⁸¹ Although we did not find any significant associations
18 between antipsychotic dose and effective connectivity parameters, only limited information on
19 medication exposure was available for this open dataset;⁴³ therefore, further investigation of the
20 specific effects of antipsychotic treatment on FST effective connectivity is warranted.

21 Our PEB analysis of the PET data identifies associations with, but not causal influences on,
22 striatal [¹⁸F]DOPA. Further investigation of patients would be required to identify precisely how effective
23 dysconnectivity of FST systems leads to dopamine dysregulation in patients. One interesting future
24 avenue of work could use effective connectivity measures to develop multivariate predictive models of
25 symptoms and dopamine synthesis capacity across different cohorts.

26 We restricted our analysis to left hemisphere FST ROIs previously implicated in past work as
27 showing disrupted functional connectivity or as being key elements of FST circuitry.^{2,3} This focus
28 facilitates efficient estimation of DCMs but may miss influences from other key regions extending
29 beyond the circuits studied here, such as the anterior cingulate cortex and anterior insula or even other
30 areas of lateral PFC or thalamus.. Recent improvements in the scalability of DCM¹⁰² may be used to
31 generate more anatomically comprehensive maps of effective dysconnectivity in psychosis.

32 **Conclusions**

33 Our analysis characterized FST effective dysconnectivity in FEP and established schizophrenia. Our
34 findings indicate that subcortical dysfunction features prominently in early illness stages, with cortical
35 abnormalities becoming more apparent later in the illness. In early psychosis, positive symptoms are
36 associated with midbrain connectivity, suggesting that aberrant bottom-up signals emanating from the

1 midbrain may present a key FST feature in the pathogenesis of psychotic symptoms. In light of other
2 findings strongly implicating cortical pathology in early illness stages,^{103,104} our results suggest that this
3 pathology may emerge after subcortical dysfunction, or that it may arise in cortical areas that were not
4 modelled in our analysis. Nigrostriatal and striatothalamic connectivity are closely linked to striatal
5 dopamine levels, while also being tied to symptom expression in patients. Together, our findings suggest
6 a prominent role for subcortical systems in driving FST dysfunction in psychosis.

7 **Acknowledgements**

8 We thank Drs Hannes Almgren and Ian Harding for advice on data analysis. The authors acknowledge
9 the facilities and scientific and technical assistance of the National Imaging Facility, a National
10 Collaborative Research Infrastructure Strategy (NCRIS) capability.

11 **Funding**

12 This work was supported by the National Health and Medical Research Council (NHMRC) (ID: 1050504),
13 Australian Research Council (ID: FT130100589) and the Charles and Sylvia Viertel Charitable Foundation.

14 Pantelis was supported by a NHMRC Senior Principal Research Fellowship (ID: 1105825). In the past 5
15 years, Pantelis served on an advisory board for Lundbeck, Australia Pty Ltd. He has received honoraria
16 for talks presented at educational meetings organized by Lundbeck.

17 M.A-J. was supported by an Investigator Grant (APP1177235) from the National Health and Medical
18 Research Council and a Dame Kate Campbell Fellowship from The University of Melbourne.

19 **Competing interests**

20 The authors declare no financial relationships with commercial interests.

21 **Supplementary material**

22 Supplementary material is available at *Brain* online.

23

1 References

- 2 1. Haber SN. Corticostriatal circuitry. *Dialogues Clin Neurosci*. 2016;18(1):7–21. doi:10.1007/978-3-
3 642-40308-8_2
- 4 2. Fornito A, Harrison BJ, Goodby E, et al. Functional dysconnectivity of corticostriatal circuitry as a
5 risk phenotype for psychosis. *JAMA psychiatry*. 2013;70(11):1143-1151.
6 doi:10.1001/jamapsychiatry.2013.1976
- 7 3. Dandash O, Fornito A, Lee J, et al. Altered striatal functional connectivity in subjects with an at-
8 risk mental state for psychosis. *Schizophr Bull*. 2014;40(4):904-913. doi:10.1093/schbul/sbt093
- 9 4. Sabaroedin K, Tiego J, Parkes L, et al. Functional connectivity of corticostriatal circuitry and
10 psychosis-like experiences in the general community. *Biol Psychiatry*. 2019;86(1):16-24.
11 doi:10.1016/j.biopsych.2019.02.013
- 12 5. Anticevic A. Understanding the role of thalamic circuits in schizophrenia neuropathology.
13 *Schizophr Res*. 2017;180:1-3. doi:10.1016/j.schres.2016.11.044
- 14 6. Pantelis C, Barnes TR, Nelson HE, et al. Frontal-striatal cognitive deficits in patients with chronic
15 schizophrenia. *Brain*. Published online 1997. doi:10.1093/brain/120.10.1823
- 16 7. Alexander GE, DeLong MR, Strick PL. Parallel organization of functionally segregated circuits
17 linking basal ganglia and cortex. *Annu Rev Neurosci*. 1986;VOL. 9:357-381.
18 doi:10.1146/annurev.ne.09.030186.002041
- 19 8. Haber SN, Fudge JL, McFarland NR. Striatonigrostriatal pathways in primates form an ascending
20 spiral from the shell to the dorsolateral striatum. *J Neurosci*. 2000;20(6):2369-2382.
21 doi:http://www.jneurosci.org/content/20/6/2369
- 22 9. Carlsson A, Waters N, Carlsson M. Neurotransmitter interactions in schizophrenia-therapeutic
23 implications. *Biol Psychiatry*. 1999;46(10):1388-1395. doi:http://dx.doi.org/10.1016/S0006-
24 3223(99)00117-1
- 25 10. Howes OD, Bose S, Turkheimer F, et al. Progressive increase in striatal dopamine synthesis
26 capacity as patients develop psychosis: a PET study. *Mol Psychiatry*. 2011;16(9):885-886.
27 doi:10.1038/mp.2011.20
- 28 11. Howes OD, Bose SK, Turkheimer F, et al. Dopamine Synthesis Capacity Before Onset of Psychosis:
29 A Prospective [18F]-DOPA PET Imaging Study. *Am J Psychiatry*. 2011;(11):1311-1317.
30 doi:10.1176/appi.ajp.2011.11010160
- 31 12. Kegeles LS, Abi-Dargham A, Frankle WG, et al. Increased synaptic dopamine function in
32 associative regions of the striatum in schizophrenia. *Arch Gen Psychiatry*. 2010;67(3):231-239.
33 doi:10.1001/archgenpsychiatry.2010.10

- 1 13. Mizrahi R, Addington J, Rusjan PM, et al. Increased stress-induced dopamine release in psychosis.
2 *Biol Psychiatry*. 2012;71(6):561-567. doi:10.1016/j.biopsych.2011.10.009
- 3 14. McGowan S, Lawrence AD, Sales T, Queded D, Grasby P. Presynaptic Dopaminergic Dysfunction
4 in Schizophrenia. *Arch Gen Psychiatry*. 2004;61(2):134. doi:10.1001/archpsyc.61.2.134
- 5 15. Allen P, Chaddock CA, Howes OD, et al. Abnormal relationship between medial temporal lobe
6 and subcortical dopamine function in people with an ultra high risk for psychosis. *Schizophr Bull*.
7 2012;38(5):1040-1049. doi:10.1093/schbul/sbr017
- 8 16. Horga G, Cassidy CM, Xu X, et al. Dopamine-Related Disruption of Functional Topography of
9 Striatal Connections in Unmedicated Patients With Schizophrenia. *JAMA Psychiatry*. 2016;10032.
10 doi:10.1001/jamapsychiatry.2016.0178
- 11 17. Woodward ND, Heckers S. Mapping thalamocortical functional connectivity in chronic and early
12 stages of psychotic disorders. *Biol Psychiatry*. 2016;79(12):1016-1025.
13 doi:10.1016/j.biopsych.2015.06.026
- 14 18. Sarpal DK, Robinson DG, Fales C, et al. Relationship between Duration of Untreated Psychosis and
15 Intrinsic Corticostriatal Connectivity in Patients with Early Phase Schizophrenia.
16 *Neuropsychopharmacology*. 2017;42(11):2214-2221. doi:10.1038/npp.2017.55
- 17 19. Wang Y, Ettinger U, Meindl T, Chan RCK. Association of schizotypy with striatocortical functional
18 connectivity and its asymmetry in healthy adults. *Hum Brain Mapp*. 2018;39(1):288-299.
19 doi:10.1002/hbm.23842
- 20 20. Kraguljac NV, White DM, Hadley N, et al. Aberrant hippocampal connectivity in unmedicated
21 patients with schizophrenia and effects of antipsychotic medication: A longitudinal resting state
22 functional mri study. *Schizophr Bull*. 2016;42(4):1046-1055. doi:10.1093/schbul/sbv228
- 23 21. Meyer-Lindenberg A, Miletich RS, Kohn PD, et al. Reduced prefrontal activity predicts
24 exaggerated striatal dopaminergic function in schizophrenia. *Nat Neurosci*. 2002;5(3):267-271.
25 doi:10.1038/nn804
- 26 22. Fusar-Poli P, Howes OD, Allen P, et al. Abnormal prefrontal activation directly related to pre-
27 synaptic striatal dopamine dysfunction in people at clinical high risk for psychosis. *Mol Psychiatry*.
28 2011;16(1):67-75. doi:10.1038/mp.2009.108
- 29 23. Modinos G, Allen P, Grace AA, McGuire P. Translating the MAM model of psychosis to humans.
30 *Trends Neurosci*. 2015;38(3):129-138. doi:10.1016/j.tins.2014.12.005
- 31 24. Howes OD, Williams M, Ibrahim K, et al. Midbrain dopamine function in schizophrenia and
32 depression: A post-mortem and positron emission tomographic imaging study. *Brain*.
33 2013;136(11):3242-3251. doi:10.1093/brain/awt264
- 34 25. Allen P, Luigjes J, Howes OD, et al. Transition to psychosis associated with prefrontal and

- 1 subcortical dysfunction in ultra high-risk individuals. *Schizophr Bull.* 2012;38(6):1268-1276.
2 doi:10.1093/schbul/sbr194
- 3 26. Hadley JA, Nenert R, Kraguljac N V., et al. Ventral tegmental area/midbrain functional
4 connectivity and response to antipsychotic medication in schizophrenia.
5 *Neuropsychopharmacology.* 2014;39(4):1020-1030. doi:10.1038/npp.2013.305
- 6 27. Weinberger DR. Implications of Normal Brain Development for the Pathogenesis of
7 Schizophrenia. *Arch Gen Psychiatry.* 1987;45(11):1055.
8 doi:10.1001/archpsyc.1988.01800350089019
- 9 28. Lodge DJ, Grace AA. Aberrant hippocampal activity underlies the dopamine dysregulation in an
10 animal model of schizophrenia. *J Neurosci.* 2007;27(42):11424-11430.
11 doi:10.1523/JNEUROSCI.2847-07.2007
- 12 29. Dempster K, Jeon P, MacKinley M, Williamson P, Théberge J, Palaniyappan L. Early treatment
13 response in first episode psychosis: a 7-T magnetic resonance spectroscopic study of glutathione
14 and glutamate. *Mol Psychiatry.* 2020;25(8):1640-1650. doi:10.1038/s41380-020-0704-x
- 15 30. Merritt K, Egerton A, Kempton MJ, Taylor MJ, McGuire PK. Nature of glutamate alterations in
16 schizophrenia a meta-analysis of proton magnetic resonance spectroscopy studies. *JAMA*
17 *Psychiatry.* 2016;73(7):665-674. doi:10.1001/jamapsychiatry.2016.0442
- 18 31. Poels EMP, Kegeles LS, Kantrowitz JT, et al. Glutamatergic abnormalities in schizophrenia: A
19 review of proton MRS findings. *Schizophr Res.* 2014;152(2-3):325-332.
20 doi:10.1016/j.schres.2013.12.013
- 21 32. Overbeek G, Gawne TJ, Reid MA, et al. Relationship Between Cortical Excitation and Inhibition
22 and Task-Induced Activation and Deactivation: A Combined Magnetic Resonance Spectroscopy
23 and Functional Magnetic Resonance Imaging Study at 7T in First-Episode Psychosis. *Biol*
24 *Psychiatry Cogn Neurosci Neuroimaging.* 2019;4(2):121-130. doi:10.1016/j.bpsc.2018.10.002
- 25 33. de la Fuente-Sandoval C, Reyes-Madrigal F, Mao X, et al. Prefrontal and Striatal Gamma-
26 Aminobutyric Acid Levels and the Effect of Antipsychotic Treatment in First-Episode Psychosis
27 Patients. *Biol Psychiatry.* 2018;83(6):475-483. doi:10.1016/j.biopsych.2017.09.028
- 28 34. Reddy-Thootkur M, Kraguljac NV, Lahti AC. The role of glutamate and GABA in cognitive
29 dysfunction in schizophrenia and mood disorders – A systematic review of magnetic resonance
30 spectroscopy studies. *Schizophr Res.* 2020;(xxxx). doi:10.1016/j.schres.2020.02.001
- 31 35. Egerton A, Modinos G, Ferrera D, McGuire P. Neuroimaging studies of GABA in schizophrenia: A
32 systematic review with meta-analysis. *Transl Psychiatry.* 2017;7(6):e1147-10.
33 doi:10.1038/tp.2017.124
- 34 36. Friston KJ, Harrison L, Penny W. Dynamic causal modelling. *Neuroimage.* 2003;19(4):1273-1302.

- 1 doi:10.1016/S1053-8119(03)00202-7
- 2 37. Friston KJ. Functional and Effective Connectivity: A Review. *Brain Connect.* 2011;1(1):13-36.
3 doi:10.1089/brain.2011.0008
- 4 38. Razi A, Kahan J, Rees G, Friston KJ. Construct validation of a DCM for resting state fMRI.
5 *Neuroimage.* 2015;106:1-14. doi:10.1016/j.neuroimage.2014.11.027
- 6 39. Dandash O, Pantelis C, Fornito A. Dopamine, fronto-striato-thalamic circuits and risk for
7 psychosis. *Schizophr Res.* 2017;180:48-57. doi:10.1016/j.schres.2016.08.020
- 8 40. Egerton A, Chaddock CA, Winton-Brown TT, et al. Presynaptic striatal dopamine dysfunction in
9 people at ultra-high risk for psychosis: Findings in a second cohort. *Biol Psychiatry.*
10 2013;74(2):106-112. doi:10.1016/j.biopsych.2012.11.017
- 11 41. Howes OD, Montgomery AJ, Asselin MC, et al. Elevated striatal dopamine function linked to
12 prodromal signs of schizophrenia. *Arch Gen Psychiatry.* 2009;66(1):13-20.
13 doi:10.1001/archgenpsychiatry.2008.514
- 14 42. Francey SM, O'Donoghue B, Nelson B, et al. Psychosocial Intervention With or Without
15 Antipsychotic Medication for First-Episode Psychosis: A Randomized Noninferiority Clinical Trial.
16 *Schizophr Bull Open.* 2020;1(1):1-11. doi:10.1093/schizbullopen/sgaa015
- 17 43. Poldrack RA, Congdon E, Triplett W, et al. A phenome-wide examination of neural and cognitive
18 function. *Sci Data.* 2016;3:1-12. doi:10.1038/sdata.2016.110
- 19 44. Leucht S, Samara M, Heres S, Davis JM. Dose Equivalents for Antipsychotic Drugs: The DDD
20 Method. *Schizophr Bull.* 2016;42(1):S90-S94. doi:10.1093/schbul/sbv167
- 21 45. Dazzi F, Shafer A, Lauriola M. Meta-analysis of the Brief Psychiatric Rating Scale – Expanded
22 (BPRS-E) structure and arguments for a new version. *J Psychiatr Res.* 2016;81:140-151.
23 doi:10.1016/j.jpsychires.2016.07.001
- 24 46. Esteban O, Markiewicz CJ, Blair RW, et al. fMRIPrep: a robust preprocessing pipeline for
25 functional MRI. *Nat Methods.* 2019;16(1):111-116. doi:10.1038/s41592-018-0235-4
- 26 47. Treiber JM, White NS, Steed TC, et al. Characterization and correction of geometric distortions in
27 814 Diffusion Weighted Images. *PLoS One.* 2016;11(3). doi:10.1371/journal.pone.0152472
- 28 48. Parkes L, Fulcher BD, Yücel M, Fornito A. An evaluation of the efficacy, reliability, and sensitivity
29 of motion correction strategies for resting-state functional MRI. *Neuroimage.* 2018;171:415-436.
30 doi:10.1016/j.neuroimage.2017.12.073
- 31 49. Pruim RHR, Mennes M, van Rooij D, Llera A, Buitelaar JK, Beckmann CF. ICA-AROMA: A robust
32 ICA-based strategy for removing motion artifacts from fMRI data. *Neuroimage.* 2015;112:267-
33 277. doi:10.1016/j.neuroimage.2015.02.064

- 1 50. Friston KJ, Kahan J, Biswal B, Razi A. A DCM for resting state fMRI. *Neuroimage*. 2014;94(August
2 2014):396-407. doi:10.1016/j.neuroimage.2013.12.009
- 3 51. Aquino KM, Fulcher BD, Parkes L, Sabaroedin K, Fornito A. Identifying and removing widespread
4 signal deflections from fMRI data: Rethinking the global signal regression problem. *Neuroimage*.
5 2020;212(February):116614. doi:10.1016/j.neuroimage.2020.116614
- 6 52. Glasser MF, Coalson TS, Bijsterbosch JD, et al. Using temporal ICA to selectively remove global
7 noise while preserving global signal in functional MRI data. *Neuroimage*. 2018;181(December
8 2017):692-717. doi:10.1016/j.neuroimage.2018.04.076
- 9 53. Hoffman JM, Melega W, Hawk T, et al. The Effects of Carbidopa Administration on Kinetics in
10 Positron Emission Tomography. *J Nucl Med*. 1992;33(8):1472-1477.
11 <https://pubmed.ncbi.nlm.nih.gov/1634937/>
- 12 54. Ruottinen HM, Rinne JO, Ruotsalainen UH, et al. Striatal [18F]fluorodopa utilization after COMT
13 inhibition with entacapone studied with PET in advanced Parkinson's disease. *J Neural Transm -*
14 *Park Dis Dement Sect*. 1995;10(2-3):91-106. doi:10.1007/BF02251225
- 15 55. Burgos N, Cardoso MJ, Thielemans K, et al. Attenuation correction synthesis for hybrid PET-MR
16 scanners: Application to brain studies. *IEEE Trans Med Imaging*. 2014;33(12):2332-2341.
17 doi:10.1109/TMI.2014.2340135
- 18 56. Baran J, Chen Z, Sforazzini F, et al. Accurate hybrid template-based and MR-based attenuation
19 correction using UTE images for simultaneous PET/MR brain imaging applications. *BMC Med*
20 *Imaging*. 2018;18(1):1-16. doi:10.1186/s12880-018-0283-3
- 21 57. Chen Z, Sforazzini F, Baran J, Close T, Shah NJ, Egan GF. MR-PET head motion correction based on
22 co-registration of multicontrast MR images. *Hum Brain Mapp*. 2019;(August 2018):1-11.
23 doi:10.1002/hbm.24497
- 24 58. Jenkinson M, Bannister P, Brady M, Smith S. Improved Optimization for the Robust and Accurate
25 Linear Registration and Motion Correction of Brain Images. 2002;841:825-841.
26 doi:10.1006/nimg.2002.1132
- 27 59. Patlak CS, Blasberg RG. Graphical evaluation of blood-to-brain transfer constants from multiple-
28 time uptake data. *J Cereb Blood Flow Metab*. 1985;5(4):584-590. doi:10.1038/jcbfm.1985.87
- 29 60. López-González FJ, Paredes-Pacheco J, Thurnhofer-Hemsi K, et al. QModeling: a Multiplatform,
30 Easy-to-Use and Open-Source Toolbox for PET Kinetic Analysis. *Neuroinformatics*.
31 2019;17(1):103-114. doi:10.1007/s12021-018-9384-y
- 32 61. Parkes L, Fulcher BD, Yücel M, Fornito A. Transcriptional signatures of connectomic subregions of
33 the human striatum. *Genes, Brain Behav*. 2017;16(7):647-663. doi:10.1111/gbb.12386
- 34 62. Diedrichsen J, Balsters JH, Flavell J, Cussans E, Ramnani N. A probabilistic MR atlas of the human

- 1 cerebellum. *Neuroimage*. 2009;46(1):39-46. doi:10.1016/j.neuroimage.2009.01.045
- 2 63. Dandash O, Harrison BJ, Adapa R, et al. Selective Augmentation of Striatal Functional
3 Connectivity Following NMDA Receptor Antagonism: Implications for Psychosis.
4 *Neuropsychopharmacology*. 2014;40(3):1-10. doi:10.1038/npp.2014.210
- 5 64. Di Martino A, Scheres A, Margulies DS, et al. Functional connectivity of human striatum: A resting
6 state fMRI study. *Cereb Cortex*. 2008;18(12):2735-2747. doi:10.1093/cercor/bhn041
- 7 65. Postuma RB, Dagher A. Basal ganglia functional connectivity based on a meta-analysis of 126
8 positron emission tomography and functional magnetic resonance imaging publications. *Cereb
9 Cortex*. 2006;16(10):1508-1521. doi:10.1093/cercor/bhj088
- 10 66. Fischl B, Salat DH, Busa E, et al. Whole brain segmentation: neurotechnique automated labeling
11 of neuroanatomical structures in the human brain. *Neuron*. 2002;33:341-355.
12 doi:10.1016/S0896-6273(02)00569-X
- 13 67. Small SA, Schobel SA, Buxton RB, Witter MP. A pathophysiological framework of hippocampal
14 dysfunction in ageing and disease. *Nat Rev Neurosci*. 2011;12(10):585-601. doi:10.1038/nrn3085
- 15 68. Zeidman P, Maguire EA. Anterior hippocampus: the anatomy of perception, imagination and
16 episodic memory. *Nat Rev Neurosci*. 2017;17(3):173-182. doi:10.1038/nrn.2015.24.Anterior
- 17 69. Murty VP, Shermohammed M, Smith D V., Carter RMK, Huettel SA, Adcock RA. Resting state
18 networks distinguish human ventral tegmental area from substantia nigra. *Neuroimage*.
19 2014;100:580-589. doi:10.1016/j.neuroimage.2014.06.047
- 20 70. Friston KJ, Litvak V, Oswal A, et al. Bayesian model reduction and empirical Bayes for group
21 (DCM) studies. *Neuroimage*. 2016;128:413-431. doi:10.1016/j.neuroimage.2015.11.015
- 22 71. Power JD, Barnes KA, Snyder AZ, Schlaggar BL, Petersen SE. Spurious but systematic correlations
23 in functional connectivity MRI networks arise from subject motion. *Neuroimage*.
24 2012;59(3):2142-2154. doi:10.1016/j.neuroimage.2011.10.018
- 25 72. Zeidman P, Jafarian A, Corbin N, et al. A guide to group effective connectivity analysis, part 1:
26 First level analysis with DCM for fMRI. *Neuroimage*. 2019;200(June):174-190.
27 doi:10.1016/j.neuroimage.2019.06.031
- 28 73. Kapur S. Psychosis as a state of aberrant salience: a framework linking biology, phenomenology,
29 and pharmacology in schizophrenia. *Am J Psychiatry*. 2003;160(1):13-23.
30 doi:10.1176/appi.ajp.160.1.13
- 31 74. McCutcheon RA, Krystal JH, Howes OD. Dopamine and glutamate in schizophrenia: biology,
32 symptoms and treatment. *World Psychiatry*. 2020;19(1):15-33. doi:10.1002/wps.20693
- 33 75. Howes OD, Kapur S. The dopamine hypothesis of schizophrenia: Version III - The final common

- 1 pathway. *Schizophr Bull.* 2009;35(3):549-562. doi:10.1093/schbul/sbp006
- 2 76. Grace AA. Dysregulation of the dopamine system in the pathophysiology of schizophrenia and
3 depression. *Nat Rev Neurosci.* 2016;17(8):524-532. doi:10.1038/nrn.2016.57
- 4 77. Maia T V., Frank MJ. An Integrative Perspective on the Role of Dopamine in Schizophrenia. *Biol*
5 *Psychiatry.* 2017;81(1):52-66. doi:10.1016/j.biopsych.2016.05.021
- 6 78. McCutcheon RA, Abi-Dargham A, Howes OD. Schizophrenia, Dopamine and the Striatum: From
7 Biology to Symptoms. *Trends Neurosci.* 2019;42(3):205-220. doi:10.1016/j.tins.2018.12.004
- 8 79. Haber SN, McFarland NR. The place of the thalamus in frontal cortical-basal ganglia circuits.
9 *Neuroscientist.* 2001;7(4):315-324. doi:10.1177/107385840100700408
- 10 80. Lodge DJ, Grace AA. Hippocampal dysregulation of dopamine system function and the
11 pathophysiology of schizophrenia. *Trends Pharmacol Sci.* 2011;32(9):507-513.
12 doi:10.1016/j.tips.2011.05.001
- 13 81. Chopra S, Francey SM, O'Donoghue B, et al. Functional Connectivity in Antipsychotic-Treated and
14 Antipsychotic-Naive Patients With First-Episode Psychosis and Low Risk of Self-harm or
15 Aggression. *JAMA Psychiatry.* Published online 2021:1-11. doi:10.1001/jamapsychiatry.2021.1422
- 16 82. Carlsson M, Carlsson A. Interactions between glutamatergic and monoaminergic systems within
17 the basal ganglia-implications for schizophrenia and Parkinson's disease. *Trends Neurosci.*
18 1990;13(7):272-276. doi:10.1016/0166-2236(90)90108-M
- 19 83. Lewis DA, Hashimoto T, Volk DW. Cortical inhibitory neurons and schizophrenia. *Nat Rev*
20 *Neurosci.* 2005;6(4):312-324. doi:10.1038/nrn1648
- 21 84. Wang AM, Pradhan S, Coughlin JM, et al. Assessing Brain Metabolism with 7-T Proton Magnetic
22 Resonance Spectroscopy in Patients with First-Episode Psychosis. *JAMA Psychiatry.*
23 2019;76(3):314-323. doi:10.1001/jamapsychiatry.2018.3637
- 24 85. Reid MA, Salibi N, White DM, Gawne TJ, Denney TS, Lahti AC. 7T Proton Magnetic Resonance
25 Spectroscopy of the Anterior Cingulate Cortex in First-Episode Schizophrenia. *Schizophr Bull.*
26 2019;45(1):180-189. doi:10.1093/schbul/sbx190
- 27 86. Sonnenschein SF, Gomes F V., Grace AA. Dysregulation of Midbrain Dopamine System and the
28 Pathophysiology of Schizophrenia. *Front Psychiatry.* 2020;11(June):1-11.
29 doi:10.3389/fpsy.2020.00613
- 30 87. Gradin VB, Waiter G, O'Connor A, et al. Salience network-midbrain dysconnectivity and blunted
31 reward signals in schizophrenia. *Psychiatry Res - Neuroimaging.* 2013;211(2):104-111.
32 doi:10.1016/j.psychres.2012.06.003
- 33 88. Winton-Brown TT, Schmidt A, Roiser JP, et al. Altered activation and connectivity in a

- 1 hippocampal-basal ganglia-midbrain circuit during salience processing in subjects at ultra high
2 risk for psychosis. *Transl Psychiatry*. 2017;7(10):1-8. doi:10.1038/tp.2017.174
- 3 89. Taylor SF, Welsh RC, Chen AC, Velander AJ, Liberzon I. Medial Frontal Hyperactivity in Reality
4 Distortion. *Biol Psychiatry*. 2007;61(10):1171-1178. doi:10.1016/j.biopsych.2006.11.029
- 5 90. Pankow A, Katthagen T, Diner S, et al. Aberrant Salience Is Related to Dysfunctional Self-
6 Referential Processing in Psychosis. *Schizophr Bull*. 2016;42(1):67-76. doi:10.1093/schbul/sbv098
- 7 91. Conio B, Martino M, Magioncalda P, et al. Opposite effects of dopamine and serotonin on
8 resting-state networks: review and implications for psychiatric disorders. *Mol Psychiatry*.
9 2020;25(1):82-93. doi:10.1038/s41380-019-0406-4
- 10 92. Cole DM, Beckmann CF, Oei NYL, Both S, van Gerven JMA, Rombouts SARB. Differential and
11 distributed effects of dopamine neuromodulations on resting-state network connectivity.
12 *Neuroimage*. 2013;78:59-67. doi:10.1016/j.neuroimage.2013.04.034
- 13 93. Makowski C, Bodnar M, Shenker JJ, et al. Linking persistent negative symptoms to amygdala-
14 hippocampus structure in first-episode psychosis. *Transl Psychiatry*. 2017;7(8).
15 doi:10.1038/tp.2017.168
- 16 94. Rajarethinam R, DeQuardo JR, Miedler J, et al. Hippocampus and amygdala in schizophrenia:
17 Assessment of the relationship of neuroanatomy to psychopathology. *Psychiatry Res -*
18 *Neuroimaging*. 2001;108(2):79-87. doi:10.1016/S0925-4927(01)00120-2
- 19 95. Walton E, Hibar DP, Van Erp TGM, et al. Prefrontal cortical thinning links to negative symptoms in
20 schizophrenia via the ENIGMA consortium. *Psychol Med*. 2018;48(1):82-94.
21 doi:10.1017/S0033291717001283
- 22 96. Sarpal DK, Robinson DG, Lencz T, et al. Antipsychotic treatment and functional connectivity of the
23 striatum in first-episode schizophrenia. *JAMA Psychiatry*. 2015;72(1):5-13.
24 doi:10.1001/jamapsychiatry.2014.1734
- 25 97. Lodge DJ, Grace AA. Divergent activation of ventromedial and ventrolateral dopamine systems in
26 animal models of amphetamine sensitization and schizophrenia. *Int J Neuropsychopharmacol*.
27 2012;15(1):69-76. doi:10.1017/S1461145711000113
- 28 98. Dandash O, Yücel M, Dagnas R, et al. Differential effect of quetiapine and lithium on functional
29 connectivity of the striatum in first episode mania. *Transl Psychiatry*. 2018;8(1).
30 doi:10.1038/s41398-018-0108-8
- 31 99. Pani SM, Sabaroedin K, Tiego J, Bellgrove MA, Fornito A. A multivariate analysis of the association
32 between corticostriatal functional connectivity and psychosis-like experiences in the general
33 community. *Psychiatry Res - Neuroimaging*. 2020;(October):111202.
34 doi:10.1016/j.pscychresns.2020.111202

- 1 100. Addington J, Chaves A, Addington D. Diagnostic stability over one year in first-episode psychosis.
2 *Schizophr Res.* 2006;86(1-3):71-75. doi:10.1016/j.schres.2006.04.018
- 3 101. Whitty P, Clark M, McTigue O, et al. Diagnostic stability four years after a first episode of
4 psychosis. *Psychiatr Serv.* 2005;56(9):1084-1088. doi:10.1176/appi.ps.56.9.1084
- 5 102. Frässle S, Harrison SJ, Heinzle J, et al. Regression dynamic causal modeling for resting-state fMRI.
6 *Hum Brain Mapp.* 2021;(January):1-22. doi:10.1002/hbm.25357
- 7 103. Seidman LJ, Thermenos HW, Poldrack RA, et al. Altered brain activation in dorsolateral prefrontal
8 cortex in adolescents and young adults at genetic risk for schizophrenia: An fMRI study of
9 working memory. *Schizophr Res.* 2006;85(1-3):58-72. doi:10.1016/j.schres.2006.03.019
- 10 104. Sun D, Phillips L, Velakoulis D, et al. Progressive brain structural changes mapped as psychosis
11 develops in “at risk” individuals. *Schizophr Res.* 2009;108(1-3):85-92.
12 doi:10.1016/j.schres.2008.11.026
- 13
14

ACCEPTED MANUSCRIPT

1 **Figure legends**

2 **Figure 1. Parent model space of fronto-striato-thalamic systems encompassing dorsal and ventral**
 3 **circuits.** Left shows anatomical locations of ROIs on axial slices. Right shows the parent model, including
 4 47 biologically plausible connections including self-connections (circular arrows) for a network
 5 comprising eight regions. Centroids of ROIs in MNI coordinates (x, y z) are presented in the bottom
 6 panel. VTA/SN: ventral tegmental area/substantia nigra (i.e., the midbrain).

7 **Figure 2. Group differences in fronto-striato-thalamic effective connectivity identified in the FEP (n =**
 8 **46), FEP-SCZ (n = 17), and SCZ (n = 36) patients relative to their respective control groups.** Differences
 9 in effective connectivity between FEP patients and healthy controls are shown in panel **(A)**, subgroup of
 10 FEP patients with schizophrenia-spectrum diagnosis are shown in panel **(B)**, and patients with
 11 established schizophrenia and healthy controls are shown in panel **(C)**. Boxes show mean connectivity
 12 values in each group. For connections between regions, dashed arrows represent connections for which
 13 patients show an increased inhibitory influence compared to controls; solid arrows represent
 14 connections for which patients show increased excitatory influence compared to controls. For self-
 15 connections, dashed arrows represent reduced inhibition and solid arrows indicate increased inhibition
 16 in patients compared to controls. Gray arrows represent modeled connections that were not
 17 significantly different from the prior. Inter-regional connectivity parameters are in Hz. Self-connection
 18 values are in negative log scale. Connections were thresholded at $P_p > 0.95$ which represents strong
 19 evidence. DC: dorsal caudate; NAcc: nucleus accumbens; VTA/SN: ventral tegmental area/substantia
 20 nigra (midbrain).

21 * denotes connections for which the mean in each group has low posterior model probability, but in
 22 which differences between groups surpassed $P_p > 0.95$.

23
 24 **Figure 3. Associations between positive symptoms and fronto-striato-thalamic effective connectivity**
 25 **parameters in the FEP (n = 46), FEP-SCZ (n = 17), and SCZ (n = 36) patients.** Panels from left to right
 26 depict the results of PEB models mapping associations between FST effective connectivity and positive
 27 symptoms in **(A)** FEP, **(B)** FEP-SCZ, and **(C)** SCZ patients. For between-region connections, solid arrows
 28 denote positive associations and dashed arrows depict negative associations between effective
 29 connectivity parameters and symptoms. For self-connections, solid arrows represent positive
 30 associations between symptom severity and self-inhibition, whereas dashed arrows denote negative
 31 associations such as more severe symptoms were associated with reduced inhibition. Gray arrows show
 32 modelled associations that were not (significantly) different from the prior. Connections were
 33 thresholded at $P_p > 0.95$. DC: dorsal caudate; NAcc: nucleus accumbens; VTA/SN: ventral tegmental
 34 area/substantia nigra (midbrain).

35 **Figure 4. Associations between fronto-striato-thalamic connectivity and striatal dopamine synthesis**
 36 **capacity.** Panel **(A)** depicts connections associated with dopamine synthesis in the dorsal circuit. Panel

1 **(B)** illustrates associations with dopamine synthesis in the ventral circuit. Solid arrows: positive
 2 associations between effective connectivity parameters and dopamine synthesis; dashed arrows:
 3 negative associations between effective connectivity parameters and dopamine synthesis; gray arrows:
 4 modelled connections that were not (significantly) different from the prior. For self-connections, solid
 5 arrows represent positive associations between striatal dopamine synthesis and self-inhibition, whereas
 6 dashed arrows denote negative associations between striatal dopamine synthesis and self-inhibition.
 7 Connections were thresholded at $P_p > 0.95$. DC: dorsal caudate; NAcc: nucleus accumbens; VTA/SN:
 8 ventral tegmental area/substantia nigra (midbrain).

10 **Table 1 Participants Descriptive Statistics**

	FEP			SCZ		[¹⁸ F]DOPA
	HC (n = 23)	FEP (n = 46)	FEP-SCZ (n = 17)	HC (n = 100)	SCZ (n = 36)	Healthy (n = 33)
Males, N (%)	14 (60.87)	20 (43.48)	9 (41.18)	55 (55)	26 (72.22)	15 (45.45)
Age, mean (SD)	21.74 (1.92)	19.12 (2.97)	20.51 (2.87)	30.6 (8.87)	35.81 (8.49)	22.30 (2.21)
Age range	18–26	15–25	15–25	21–50	22–49	18–28
BPRS Total						
Mean (SD)	–	56.91 (10.34)	61.94 (9.41)	–	49.39 (14.03)	–
Range	–	38–80	46–80	–	26–77	–
BPRS Positive						
Mean (SD)	–	15.65 (4.19)	17.94 (4.31)	–	14.11 (6.17)	–
Range	–	10–27	13–27	–	5–29	–
BPRS Negative						
Mean (SD)	–	5.76 (2.6)	7 (3.16)	–	5.14 (2.54)	–
Range	–	3–12	3–12	–	3–11	–

11 FEP: first-episode psychosis group; FEP-SCZ: first-episode psychosis subgroup with a diagnosis of schizophrenia spectrum disorder; SCZ:
 12 schizophrenia group; HC: healthy controls; [¹⁸F]DOPA: healthy group who underwent a simultaneous PET-fMRI protocol
 13

14

1 **Table 2 Summary of Group Differences in Fronto-striato-thalamic Effective Connectivity in FEP (n = 46), FEP-SCZ (n = 17),**
 2 **and SCZ (n = 36) Patients Respective to Healthy Controls**

Connection	Increased (+) or decreased (-) in patients	Excitatory (E) or inhibitory (I) in patients	Effect size (Hz)	90% Posterior Confidence Interval (lower bound, upper bound)	Patients (mean)	Controls (mean)
FEP vs HCs						
<i>dIPFC → dIPFC</i>	+	E	0.10	0.03, 0.20	0.64	0.44
Thal → NAcc	-	I	0.10	-0.20, -0.01	-0.12	0.09
Amyg → NAcc	+	E	0.11	0.02, 0.21	0.00	-0.24
<i>VTA/SN → VTA/SN</i>	-	I	0.14	-0.24, -0.04	-0.04 (-0.48)	0.00 (-0.05)
FEP-SCZ vs HCs						
Thal → NAcc	-	I	0.13	-0.24, -0.03	-0.13	0.09
Amyg → NAcc	+	E	0.13	0.02, 0.23	0.00	-0.25
<i>Amyg → Amyg</i>	-	I	0.11	-0.22, 0.00	-0.16 (-0.43)	0.00 (-0.05)
NAcc → Hipp	-	I	0.15	-0.26, -0.04	-0.28	0.00
<i>VTA/SN → Hipp</i>	-	I	0.09	-0.20, -0.02	-0.14	0.00
<i>VTA/SN → NAcc</i>	+	E	0.09	-0.01, 0.20	0.00	-0.14
<i>VTA/SN → VTA/SN</i>	-	I	0.08	-0.19, 0.03	-0.06* (-0.47)	0.07* (-0.54)
SCZ vs HCs						
<i>dIPFC → Thal</i>	-	I	0.11	-0.19, -0.03	-0.14	0.00
<i>vmPFC → dIPFC</i>	-	I	0.08	-0.16, 0.00	-0.06*	0.06*
Thal → Hipp	-	I	0.10	-0.18, -0.02	-0.20	0.00
Thal → NAcc	-	I	0.09	-0.17, -0.01	-0.11	0.00
Amyg → Hipp	-	E	0.09	-0.17, -0.01	0.00	0.16
<i>VTA/SN → VTA/SN</i>	-	I	0.16	-0.25, -0.07	-0.26 (-0.39)	-0.09 (-0.46)
<i>VTA/SN → DC</i>	-	I	0.14	-0.22, -0.06	-0.19	0.00
<i>DC → VTA/SN</i>	+	E	0.16	0.08, 0.25	0.12	-0.11

3 FEP: first-episode psychosis group; FEP-SCZ: first-episode psychosis subgroup with a diagnosis of schizophrenia spectrum disorder; SCZ:
 4 schizophrenia group; HC: healthy controls. Only connections surpassing a posterior probability threshold of 0.95 are presented in this table,
 5 and all reported connections have the posterior probability value of 1.00. All parameters for between region connections are in Hz.
 6 Self-connections are italicized, and values are log-transformed to ensure prior negativity (i.e., inhibitory) constraints on self-connections. A
 7 positive value for self-connection denotes increased inhibition, a negative value signifies reduced inhibition. Self-connection parameters in Hz
 8 are displayed in parentheses.

9 *Denotes connections for which the mean in each group has low posterior model probability, but in which differences between groups
 10 surpassed $P_p > 0.95$.

11
12
13

1 **Table 3 Summary of Connections Associated with Severity of Positive Symptoms in FEP (n = 46), FEP-SCZ (n = 17), and SCZ**
 2 **(n = 36) Patients**

Connection	Positive (+) or negative (-) association	Effect size (Hz)	90% Posterior Confidence Interval (lower bound, upper bound)
Positive symptoms			
FEP			
dIPFC → vmPFC	-	0.10	-0.20, 0.01
vmPFC → vmPFC	-	0.16	-0.27, -0.06
Amyg → Amyg	-	0.08	-0.19, 0.02
Hipp → VTA/SN	+	0.10	0.00, 0.20
NAcc → VTA/SN	+	0.09	-0.01, 0.20
VTA/SN → NAcc	+	0.09	-0.02, 0.20
VTA/SN → Hipp	-	0.17	-0.27, -0.06
VTA/SN → Amyg	+	0.14	0.04, 0.25
VTA/SN → DC	-	0.08	-0.19, 0.02
FEP-SCZ			
vmPFC → vmPFC	-	0.19	-0.33, -0.05
dIPFC → dIPFC	-	0.09	-0.23, 0.04
dIPFC → Thal	+	0.11	-0.02, 0.24
Thal → Thal	+	0.13	0.00, 0.26
Hipp → Amyg	-	0.15	-0.28, -0.02
NAcc → Hipp	-	0.09	-0.22, 0.03
NAcc → VTA/SN	+	0.12	-0.01, 0.25
DC → Thal	-	0.12	-0.25, 0.02
VTA/SN → NAcc	+	0.13	0.01, 0.26
VTA/SN → Hipp	-	0.14	-0.27, -0.01
VTA/SN → Amyg	+	0.10	-0.03, 0.23
VTA/SN → DC	-	0.12	-0.25, 0.01
SCZ			
vmPFC → vmPFC	-	0.09	-0.20, 0.03
vmPFC → Hipp	+	0.16	0.05, 0.27
vmPFC → VTA/SN	+	0.08	-0.03, 0.20
dIPFC → dIPFC	+	0.09	-0.03, 0.21
dIPFC → Thal	-	0.18	-0.24, -0.06
Thal → Hipp	+	0.11	0.00, 0.22
Thal → VTA/SN	-	0.13	-0.24, -0.02
Hipp → vmPFC	-	0.09	-0.21, 0.02
DC → Thal	+	0.08	-0.03, 0.19
VTA/SN → VTA/SN	-	0.15	-0.27, -0.04
VTA/SN → Amyg	-	0.10	-0.21, 0.01
VTA/SN → dIPFC	+	0.11	0.00, 0.21

3 FEP: first-episode psychosis group; FEP-SCZ: first-episode psychosis subgroup with a diagnosis of schizophrenia spectrum disorder; SCZ:
 4 schizophrenia group

5 Only connections surpassing a posterior probability threshold of 0.95 are presented in this table, and all reported connections have the
 6 posterior probability value of 1.00.

7 All parameters for between region connections are in Hz. Self-connections are italicized, and values are log-transformed to ensure prior
 8 negativity (i.e., inhibitory) constraints on self-connections. A positive value for self-connection denotes increased inhibition, a negative value
 9 signifies reduced inhibition. Positive symptoms measured with BPRS Positive subscale.
 10
 11

1 **Table 4 Summary of Connections Associated with Striatal Dopamine Synthesis**

Connection	Positive (+) or negative (-) association	Effect size (Hz)	90% Posterior Confidence Interval (lower bound, upper bound)
Dorsal Striatum			
<i>Thal → Thal</i>	+	<i>0.10</i>	-0.04, 0.23
Thal → DC	+	0.09	-0.04, 0.22
Thal → VTA/SN	+	0.12	-0.01, 0.26
Amyg → vmPFC	+	0.08	-0.05, 0.21
Amyg → Thal	+	0.11	-0.02, 0.24
DC → Thal	-	0.13	-0.26, 0.00
Ventral Striatum			
Hipp → Thal	+	0.16	0.03, 0.30
Hipp → VTA/SN	+	0.16	0.03, 0.29
Amyg → Thal	-	0.12	-0.25, 0.02
NAcc → Thal	-	0.11	-0.24, 0.02
<i>Amyg → Amyg</i>	-	<i>0.14</i>	<i>-0.27, 0.01</i>
<i>NAcc → NAcc</i>	-	<i>0.14</i>	<i>-0.28, 0.00</i>
DC → VTA/SN	-	0.12	-0.25, 0.01
DC → DC	+	<i>0.10</i>	<i>-0.03, 0.22</i>
VTA/SN → VTA/SN	+	<i>0.10</i>	<i>-0.05, 0.25</i>
VTA/SN → vmPFC	+	0.15	0.02, 0.29
VTA/SN → DC	+	0.12	-0.01, 0.25

2 Only connections surpassing a posterior probability threshold of 0.95 are presented in this table, and all reported connections have the
3 posterior probability value of 1.00.

4 All parameters for between region connections are in Hz. Self-connections are italicized, and values are log-transformed to ensure prior
5 negativity (i.e., inhibitory) constraints on self-connections. A positive value for self-connection denotes increased inhibition, a negative value
6 signifies reduced inhibition.
7

8

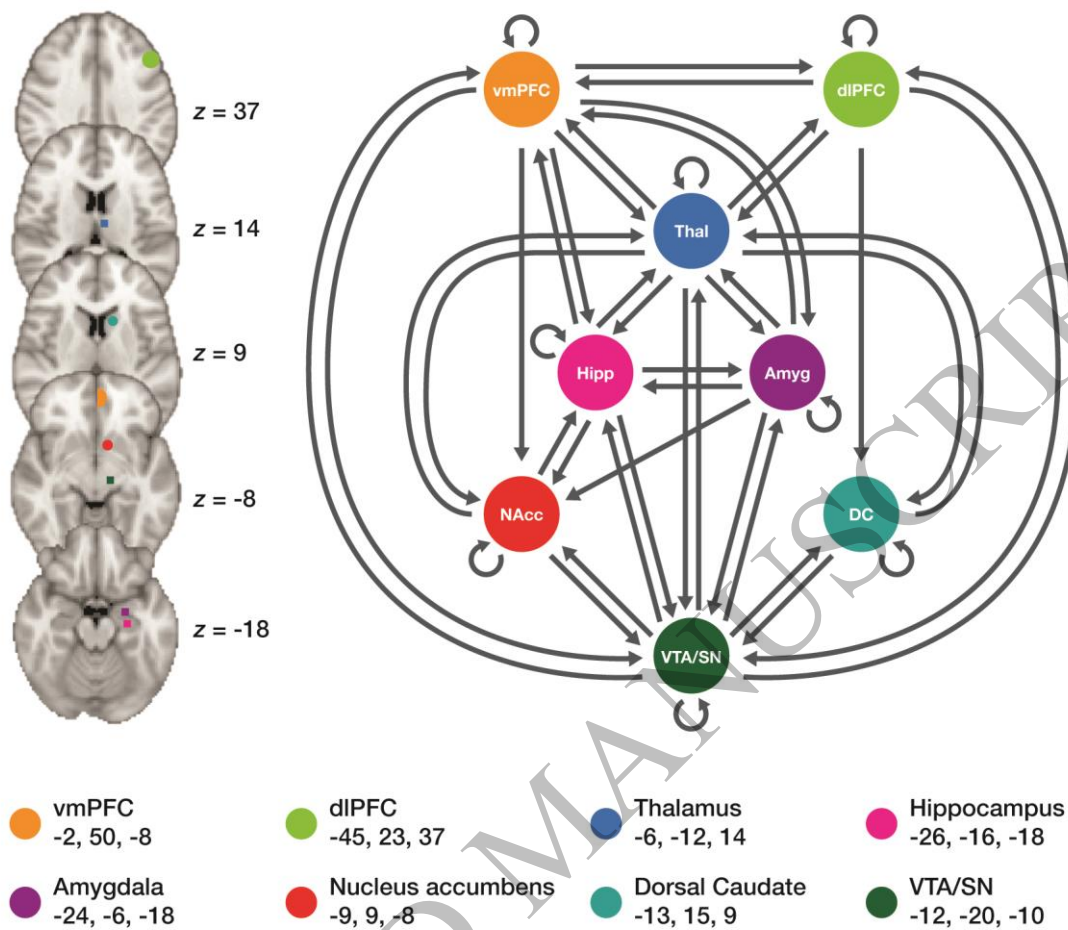


Figure 1
156x134 mm (71 x DPI)

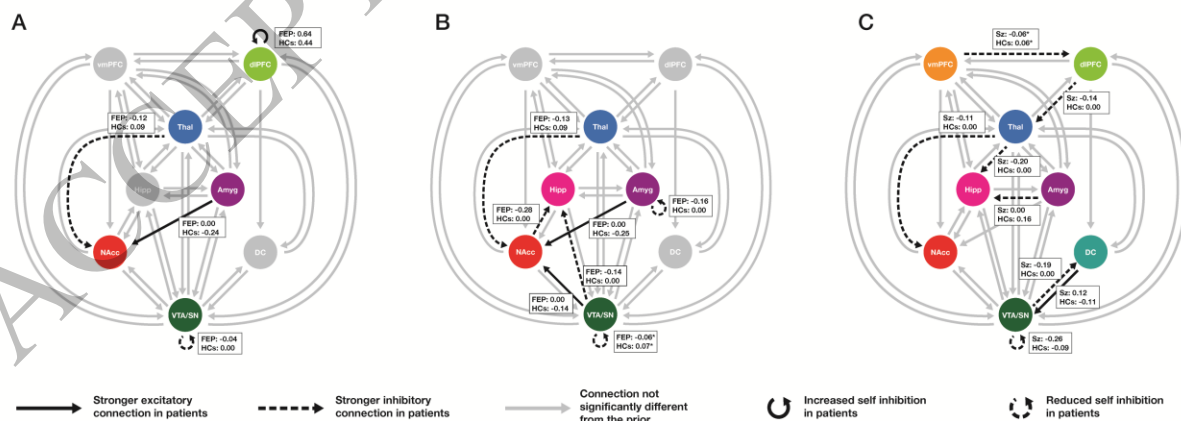


Figure 2
319x119 mm (71 x DPI)

1
2
3

4
5
6

1

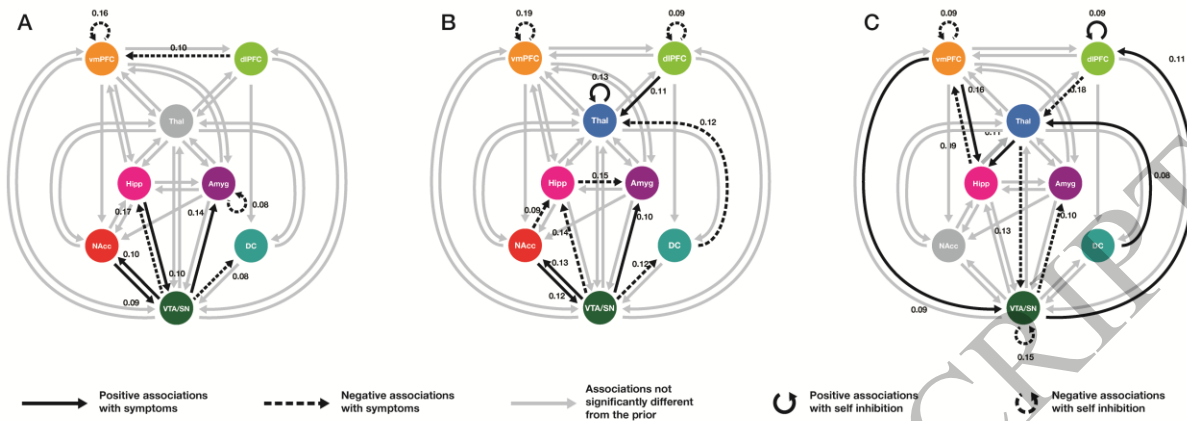


Figure 3
319x119 mm (71 x DPI)

2
3
4
5

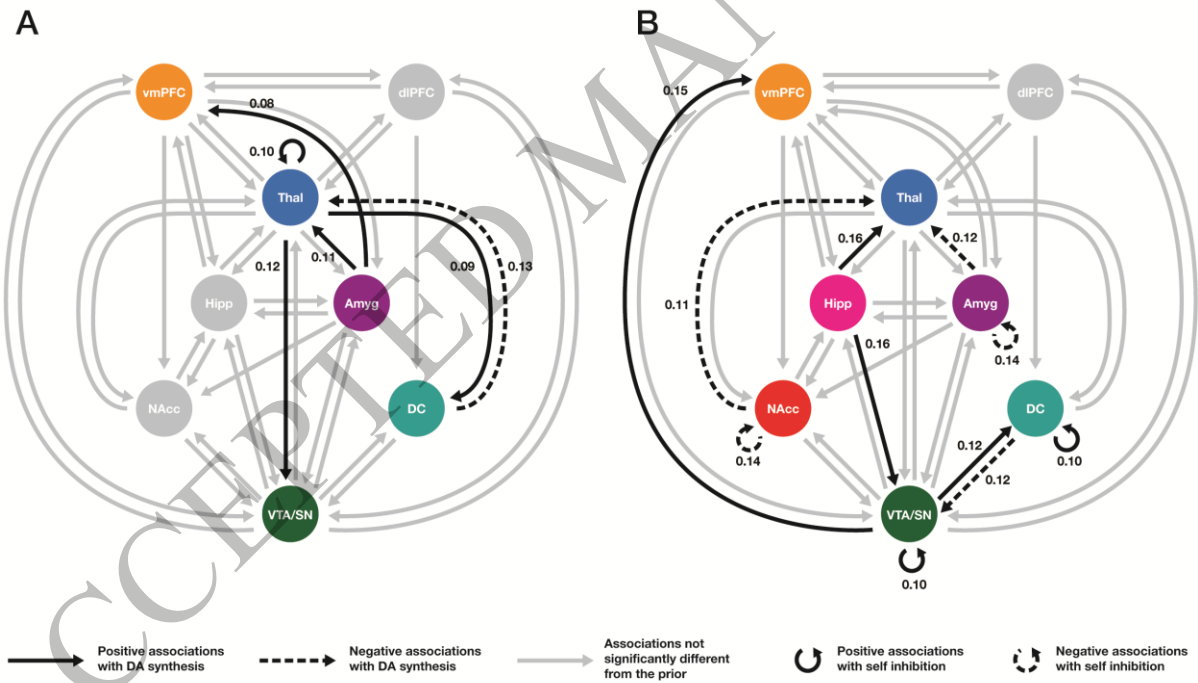


Figure 4
210x127 mm (71 x DPI)

6
7
8